PHYSICAL REVIEW B **96**, 100506(R) (2017)

Tuning pairing amplitude and spin-triplet texture by curving superconducting nanostructures

Zu-Jian Ying,[1,2] Mario Cuoco,[1] Carmine Ortix,[3,4] and Paola Gentile[1]

[1]*CNR-SPIN and Dipartimento di Fisica "E. R. Caianiello", Università di Salerno, I-84084 Fisciano (Salerno), Italy*

[2]*Beijing Computational Science Research Center, Beijing 100084, China*

[3]*Institute for Theoretical Physics, Center for Extreme Matter and Emergent Phenomena, Utrecht University, Princetonplein 5, 3584 CC Utrecht, The Netherlands*

[4]*Institute for Theoretical Solid State Physics, IFW-Dresden, Helmholtzstraße 20, D-01069 Dresden, Germany*

(Received 28 March 2017; published 20 September 2017)

We investigate the nature of the superconducting (SC) state in curved nanostructures with Rashba spin-orbit coupling (RSOC). In bent nanostructures with inhomogeneous curvature we find a local enhancement or suppression of the SC order parameter, with the effect that can be tailored by tuning either the RSOC strength or the carrier density. Apart from the local SC spin-singlet amplitude control, the geometric curvature generates nontrivial textures of the spin-triplet pairs through a spatial variation of the $\vec{d}$ vector. By employing the representative case of an elliptical quantum ring, we demonstrate that the $\vec{d}$ vector strongly depends on the local curvature and it generally exhibits a three-dimensional profile whose winding is tied to that of the single electron spin in the normal state. Our findings unveil paths to manipulate the quantum structure of the SC state in RSOC nanostructures through their geometry.

DOI: 10.1103/PhysRevB.96.100506

Introduction. Inversion symmetry breaking is a fundamental property that yields spin-orbit locking and sets the structure of both single electron and paired quantum states. Indeed, on the one hand, for low-dimensional semiconducting nanosystems with structure inversion asymmetry, the Rashba spin-orbit coupling (RSOC) [1–3] allows one to tune the spin orientation through the electron propagation and vice versa to exert a spin control on the electron trajectories. On the other hand, lack of inversion symmetry in superconductors makes neither spin nor parity good quantum numbers anymore. The ensuing mixing of even spin-singlet (SS) and odd spin-triplet (ST) channels [4,5] leads to a series of novel features ranging from the anomalous magnetoelectric [6] effect, to unconventional surface states [7], and topological phases [8,9]. A major boost in the framework of inversion asymmetric systems relied on the proposal [10,11] and the observation of a topological superconducting (SC) phase [12–15], hosting end Majorana modes, in a one-dimensional (1D) semiconductor nanowire with sizable RSOC and proximity-induced superconductivity. Although the investigation of Majorana modes primarily focuses on single semiconducting wires, Majorana detection and braiding often require more complex networks [16–18] or suggest alternative curved geometries, e.g., circular [19–22] and elliptical quantum rings [23].

The study of RSOC semiconducting rings has opened the path to a geometric design of the electron spin and quantum geometric phase as predicted [24,25] and experimentally demonstrated through the application of an external magnetic field [26]. Recently, the theoretical analysis of shape-deformed RSOC nanostructures established a deep connection between electronic spin textures, spin transport properties, and the nanoscale shape of the system, thus providing foundational elements for an all-geometrical and electrical control of the spin orientation [27], including the possibility of topological nontrivial phases [27,28]. Along this line, due to the expected strong impact of inversion symmetry breaking on single and paired electronic states, fundamental questions naturally arise on the character of the superconducting state in RSOC shape deformed superconductors or curved semiconductor-superconductor heterostructures.

The delicate interplay between geometry and condensed matter order has a broad framework [29] and for the case of superconductivity can lead to distinct physical effects when considering, for instance, the role of dislocations with conventional [30,31] or unconventional pairing [32], the samples geometry [33], the modification of the proximity behavior [34], as well as the occurrence of novel quantum phases in confined structures [35]. In this Rapid Communication, we aim to unveil the interplay between shape deformations and superconductivity in RSOC nanostructures. While in systems with constant curvature (e.g., quantum wires or circular rings) the RSOC is monotonously affecting the superconductivity, the spatial variation of the Rashba field through the curvature of the nanostructure can twist the effective electron mass such as to yield either a local enhancement or a suppression of the SC order parameter (OP). We demonstrate this effect by employing elliptically shaped quantum rings and we provide evidence for its control through both the RSOC and electron density. Apart from driving the SC-SS amplitude, the inhomogeneous profile of the curvature generates nontrivial spatial patterns of the ST pairs. We show that the geometric curvature can tailor the ST pairing by yielding three-dimensional spatial textures, and the behavior of the $\vec{d}$ vector generally follows the evolution of the electron spin orientation in the normal state. Such findings indicate that the curvature can effectively yield a spin torque on the electron spin pairs.

Model. We consider electrons moving along a 1D planarly curved nanostructure (Fig. 1) in the presence of a local SS pairing interaction. Due to the structural inversion symmetry breaking the electrons are subject to a RSOC, which, as in the case of a not-curved nanostructure [Fig. 1(a)], couples the orbital and the local spin component normal to the electron motion [36]. Since the nanostructure has a nontrivial geometric profile, the spin orientation perpendicular to the

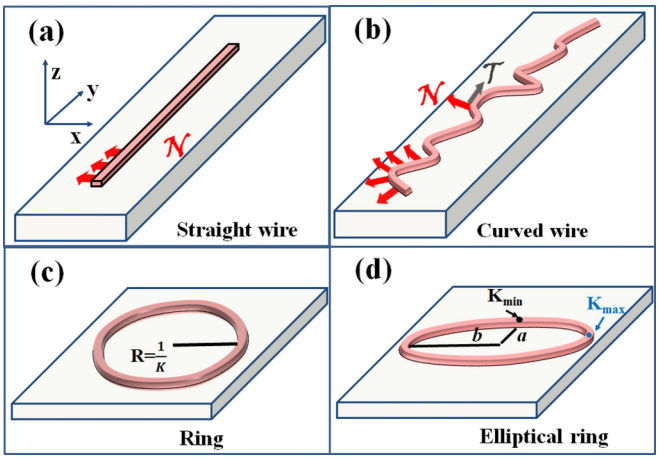

FIG. 1. Schematics of the geometric profile of (a) straight, (b) planarly curved nanostructure, (c) ring, and (d) elliptically deformed ring with semiaxes a and b. Red (gray) arrows indicate the perpendicular (tangential) direction of the spin orientation. K is the curvature of the ring, e.g., the inverse of its radius R. Black (blue) dots indicate a position with minimum $K_{\min}$ (maximal $K_{\max}$) amplitude of the curvature in the elliptical ring, respectively.

momentum of the quasiparticle changes its direction and thus it is spatially dependent. Such aspect can be conveniently expressed by introducing the local normal $\hat{\mathcal{N}}(s)$ and tangential $\hat{\mathcal{T}}(s)$ directions at a given position s along the curve, as well as the corresponding local Pauli matrices for the spin components, i.e., $\sigma_N(s) = \boldsymbol{\tau} \cdot \hat{\mathcal{N}}(s)$ and $\sigma_T(s) = \boldsymbol{\tau} \cdot \hat{\mathcal{T}}(s)$ in the moving frame of the electrons, with $\boldsymbol{\tau}$ being the usual Pauli matrices [Fig. 1(a)]. Then, the Bogoliubov–de Gennes (BdG) Hamiltonian [37] for a planar nonuniformly curved nanostructure with RSOC [27,28,36,38,39] and local pairing interaction can be written as

$$\mathcal{H} = \int ds\, c_\sigma^\dagger(s)\left\{\left(-\frac{\hbar^2}{2m^\star}\partial_s^2 - \mu\right) + \frac{i\alpha_{SO}}{2}[\sigma_N(s)\partial_s + \partial_s\sigma_N(s)]\right\}c_{\sigma'}(s) + [\Delta(s)c_\uparrow^\dagger(s)c_\downarrow^\dagger(s) + \text{H.c.}] + \frac{|\Delta(s)|^2}{g},$$

where $c_\sigma^\dagger(s)$ creates an electron with spin σ at the position s, being the arclength of the planar curve measured from an arbitrary reference point, $m^\star$ is the effective mass of the charge carriers, α_{SO} is the RSOC, g is the interaction in the spin-singlet channel, and μ stands for the chemical potential. The amplitude $\Delta(s) = g\langle c_\uparrow(s)c_\downarrow(s)\rangle$ indicates the expectation value on the ground state of the local SS-OP, and it is determined self-consistently until the minimum of the free energy is achieved within the desired accuracy. $\mathcal{H}$ generalizes the Hamiltonian originally proposed for a quantum ring with constant curvature [40] and includes an inhomogeneous curvature profile, as well as a local SS pairing coupling. For a bent nanowire [Fig. 1(b)], the normal and tangential directions to the curve can be expressed in terms of a polar angle $f(s)$ as $\hat{\mathcal{N}}(s) = \{\cos f(s), \sin f(s), 0\}$, and $\hat{\mathcal{T}}(s) = \{\sin f(s), -\cos f(s), 0\}$. The polar angle is related to the local curvature $K(s)$ via $\partial_s f(s) = -K(s)$. To compute the spatial dependent pairing amplitude we follow the conventional mapping of the Hamiltonian from continuum

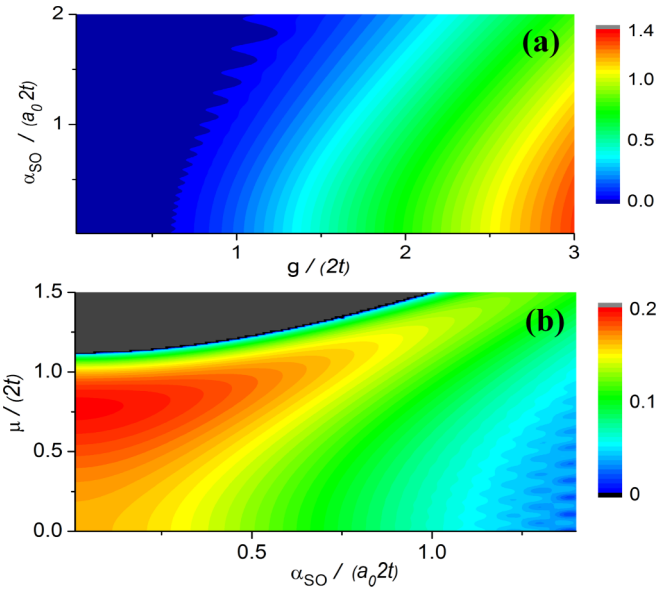

FIG. 2. Contour map of the averaged spin-singlet OP for a ring ($L = 100$ sites) by varying the electron density via μ, the RSOC α_{SO}, and the SC coupling g. a_0 is the interatomic distance and t the nearest-neighbor hopping amplitude. In (a) $\mu = 0$ (half-filling) and $g/(2t) = 1.0$ in (b).

to lattice [27,28,37] and solve the BdG equations [41]. The analysis has been performed for systems size up to $L = 400$ sites. Greater values do not change qualitatively the results [37].

Phase diagram. We start by comparing the cases of a quantum wire, a circular, and an elliptical ring. The aim is to establish which role the shape plays in tailoring the superconducting OP. Remarkably, we find a sort of universal behavior for the averaged OP over the length of the system when comparing different shapes. Indeed, the tendency is to have a detrimental impact on the SC state by increasing the RSOC, due to a bandwidth broadening and large spin split of the bands, with a critical threshold above which a significant suppression of superconductivity occurs. The threshold is dependent on g, such as larger values of α_{SO} are needed to suppress the SC state when moving from a weakly to a strongly coupled regime [Fig. 2(a)]. The phase diagram for different electron filling indicates that the most favorable conditions for the superconductivity are obtained when the Fermi level is close to the band edge (i.e., $\mu \sim 2t$), consistently with the position of the maximum of the density of states due to the 1D hopping connectivity. When α_{SO} becomes comparable with t, the SC state can survive in a broader region of μ due to the bandwidth enlargement by the RSOC [Fig. 2(b)].

Inhomogeneous spatial profile of the spin-singlet OP. The elliptically deformed ring [Fig. 1(d)] is an ideal platform to explore the consequences of the curvature because the imbalance of the semiaxis lengths naturally introduces a gradient of the curvature and two different regions with a larger (smaller) curvature strength [Fig. 1(c)]. An inspection of the local OP indicates an intricate interrelation among its variation, the spatial dependent curvature, and the RSOC (Fig. 3). As a consequence of the Rashba field bending, indeed, the OP gets

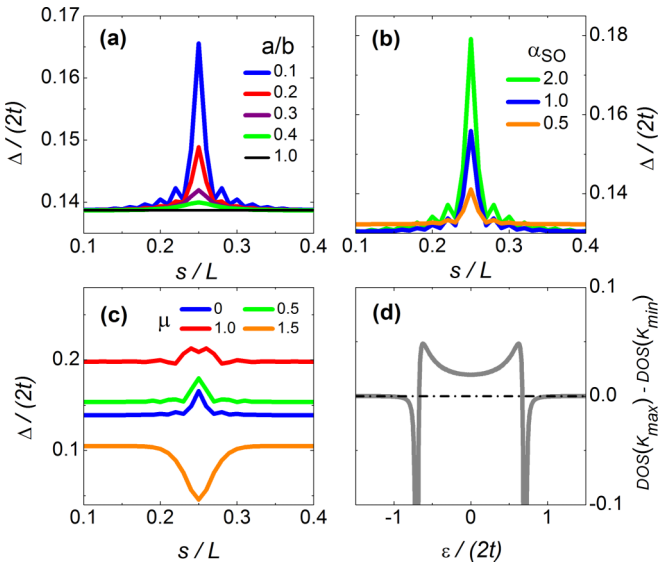

FIG. 3. Spin-singlet OP close to the maximal curvature ($K_{\max}$) (i.e., $s/L = 0.25$) in the elliptical ring as a function of (a) a/b, (b) the RSOC, and (c) the chemical potential. (d) Difference between the local density of states at $K_{\max}$ and $K_{\min}$ in the elliptical ring (see Fig. 1). Microscopic parameters are (a) $\mu = 0.0, \alpha_{SO} = 1.0, g = 1.2$; (b) $a/b = 0.1$, $\mu = 0.0$, $g = 1.0, 1.18, 1.66$ for $\alpha_{SO} = 0.5, 1.0, 0.5$, respectively. In (c) $\alpha_{SO} = 1.0$, $a/b = 0.1$, $g = 1.2$. For (d) we have $\alpha_{SO} = 1.0$, $a/b = 0.1$. All the energies are in units of $2t$.

enhanced or suppressed in the region where the curvature is maximal and strongly inhomogeneous [e.g., nearby $K_{\max}$ in Fig. 1(d)], and the strength of the variation can be controlled through the ratio a/b [Fig. 3(a)] and the RSOC [Fig. 3(b)]. We find that the OP amplitude depends on the electron density in the nanostructure [Fig. 3(c)], namely, it increases close to half-filling while it gets suppressed or enhanced in the low- (high-) density regime when the chemical potential is close to the band edge. There are two main sources for the curvature-induced OP variation. First, a spatial modification of the local Rashba field is generally expected to induce a local conversion of SS into ST pairs that would result in a reduction of the SS-OP when comparing the uniform with the inhomogeneous curvature profiles. However, the spatial ST correlations are not much affected by a change in the electron density. Therefore, such mechanism can be ruled out as a primary origin of the SS-OP variation. On the other hand, a closer view of the local density of states (LDOS) in the normal state reveals that a change of the energy spectrum close to the Fermi level affects the strength of the SC-OP. Indeed, this is observed when comparing the computed spatial dependent DOS along the elliptical loop at positions of maximum ($K_{\max}$) and minimum ($K_{\min}$) curvature, as demonstrated in Fig. 3(d). We find that the LDOS at $K_{\max}$ is always enhanced with respect to $K_{\min}$ except when the Fermi level is close to the band edge. The consequence on the SC amplitude follows the expectation of the BCS theory that a larger DOS at the Fermi level yields a stronger OP amplitude. We notice that, even for a SC coherence length ξ that is comparable to the ring's length L, the local OP undergoes similar spatial modulations [37]. One additional remark concerns the averaged OP for a generic shape of the SC nanostructure. Since the integrated curvature of a single loop curved nanostructure is constrained to be 2π, an enhancement in a given region should be compensated by a suppression in another one, thus, driving a cancellation in the spatial average of the OP. However, if the curvature changes sign (e.g., for a wrinkled profile) the cancellation would be less effective, because the OP is not sensitive to the sign of the curvature [37].

Spatial texture of the ST pairing amplitude. Since the bending of the RSOC nanostructure can torque the spin orientation [42] with windings around z and $\hat{\mathcal{N}}$ [27], the SC state is prone to exhibit ST correlations with nontrivial textures in space. It is convenient to introduce the ST correlator in real space in terms of a bond $\vec{d}(s_i)$-vector component along the symmetry axes of the elliptical ring as $d_x(s_i) = \frac{1}{2}(-\langle c_\uparrow(s_i)c_\uparrow(s_i + a_0)\rangle + \langle c_\downarrow(i)c_\downarrow(i + a_0)\rangle)$, $d_y(s_i) = \frac{i}{2}(\langle c_\uparrow(s_i)c_\uparrow(s_i + a_0)\rangle + \langle c_\downarrow(s_i)c_\downarrow(s_i + a_0)\rangle)$, and $d_z(s_i) = (\langle c_\uparrow(s_i)c_\downarrow(s_i + a_0) + \langle c_\downarrow(s_i)c_\uparrow(s_i + a_0)\rangle)$, with s_i labeling the ith site of the curved nanowire and a_0 the interatomic distance. In noncentrosymmetric or surface superconductivity, the RSOC marks the lack of inversion center through a vector $\vec{l}_k$ [5]. There, the ST pairing is not excluded [5] and an optimal configuration is for $\vec{d}_k || \vec{l}_k$ [5]. Here, we deal with a spatial variation of the Rashba field, and we focus on the regime where the RSOC is larger than the SC gap. As expected, for the uniform wire the $\vec{d}$ vector lies in the plane of the 1D system [Fig. 4(e)], and is collinear to $\mathcal{N}$ [Fig. 1(a)] and the electron spin orientation $\vec{\sigma}$ associated with one of the Kramers degenerate states at the Fermi level [Fig. 4(a)]. A ring with a constant curvature introduces a nontrivial z component both for $\vec{\sigma}$ [Fig. 4(b)] and in the $\vec{d}$ pattern [Fig. 4(f)] due to the spin torque induced by the geometric curvature [42]. Although the curvature is constant and uniform, the SC behavior is different from the chain as the $\vec{d}$ vector has an out-of-plane z component and is not collinear to $\vec{\sigma}$. For the elliptical ring, we find a three-dimensional $\vec{d}$ pattern that is modulated in amplitude and orientation when moving from a region with large to small curvature [Figs. 4(g) and 4(h)]. Different types of spatial profiles occur depending on the character of the electron spin pattern in the normal state. Indeed, when $\vec{\sigma}_z$ and $\vec{\sigma}_T$ change sign, also $\vec{d}$ manifests a similar variation [Figs. 4(g) and 4(h)]. Thus, remarkably, the $\vec{d}$ vector has a complete winding around $\hat{\mathcal{N}}$ [Figs. 4(g) and 4(h)] thereby following that of $\vec{\sigma}$ in the normal state [Figs. 4(c) and 4(d)]. Apart from the winding around z which is due to the loop geometry, the $\vec{d}$ vector provides evidence for the occurrence of topologically nontrivial quantum states in all regimes of electron spin texture. Interestingly, we find that the $\vec{d}$ modulation in amplitude and orientation [Fig. 4(h)] is stronger when in the normal state the spin texture has both windings around z and $\hat{\mathcal{N}}$ directions [Fig. 4(d)]. A consequence of such texture is that a supercurrent spin flow is generated by the $\vec{d}$ spatial gradient. Indeed, when considering the interface of two noncollinear $\vec{d}_i$ and $\vec{d}_j$, a spin current flows across it with a spin orientation $\vec{n} = \vec{d}_i \times \vec{d}_j$ [43]. For a $\vec{d}$ winding around $\hat{\mathcal{N}}$, d_z changes smoothly from $+z$ to $-z$ and again from $-z$ to $+z$ when encircling the ring. Hence, one has

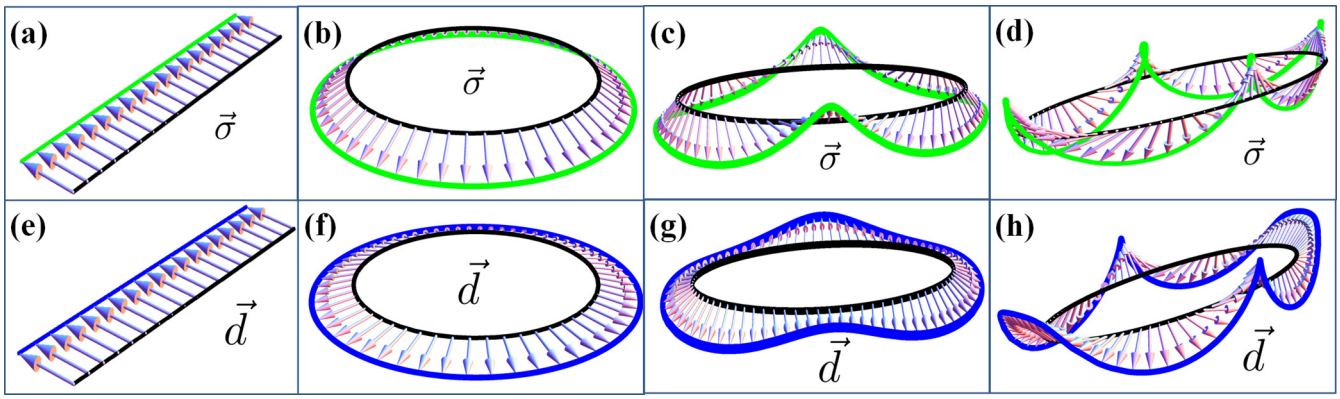

FIG. 4. Electron spin orientation $\vec{\sigma}$ in the normal state (i.e., $g = 0$) for the wire (a), ring (b), and elliptical ring in (c) and (d). (c) and (d) are for the electron spin with a winding around $\mathcal{N}$ and $\mathcal{N}$-z directions. The $\vec{d}$ vector in (e), (f), (g), and (h) correspond to the spin patterns in (a), (b), (c), and (d), respectively. In the SC state we have $g = 0.5$ and $\mu = 0.5$ for all the geometrical configurations, i.e., (e)–(h). The RSOC is $\alpha_{SO} = 0.053$ for the wire and the ring. For the elliptical ring the RSOC is $\alpha_{SO} = 0.085$ in (c) and (g), while $\alpha_{SO} = 0.12$ is chosen for (d) and (h). The configurations for the elliptical ring are for $a/b = 0.3$. All the energy scales are in units of $2t$.

a formation of $\vec{d}$-soliton–antisoliton pairs that are associated with a $\vec{d}$ phase slip of $\pm\pi$. Breaking the d-soliton–antisoliton pairs (e.g., through an applied magnetic field) can lead to configurations with a single π slip of the $\vec{d}$ vector when encircling the ring. In this circumstance, the spin phase slip is accompanied by an orbital π shift that results in a half-integer flux quantum configuration with a topological nature [44,45] and non-Abelian statistics [46].

Conclusions. To wrap up, we demonstrated two main effects: (i) the amplitude of the SS-OP can be manipulated by curvature and (ii) the ST $\vec{d}$ vector exhibits winding along the curved profile. We point out that for (i) the effect can become significant when the squeezing ratio a/b is less than about 0.3 and for a RSOC that is of the order of the hopping amplitude, being not significantly dependent on the pairing interaction in the weak-coupling regime. With regard to (ii), the winding of the $\vec{d}$ vector generally occurs when the squeezing ratio a/b is below about 0.5 with a weak dependence on the strength of the RSOC. An immediate consequence of our results is that the geometric change of the OP can be employed to engineer junctions with regions of enhanced or suppressed superconductivity integrated in a single material system and, in turn, to suitably tailor the transport properties. A key experimental setup for probing the correlation between geometry and superconductivity would be to prepare nanorings with elliptical shape and measure the OP spatial amplitude variation by directly accessing the LDOS through scanning tunneling microscopy. Since RSOC strength is large on the surface states of high Z metals, such as Au [47], Bi [48], and Pb [49], feasible platforms might be based on lithographically designed asymmetric nanorings of these materials. Other candidates are the quasi-1D quantum wells at LAO-STO interface [50–52] or similar oxides where RSOC is strong, gate tunable, and the shape design can be achieved not only by nanolithography but also by electrical means. For the aforementioned materials and configurations, the occurrence of a $\vec{d}$ texture can be primarily investigated through a measurement of magnetization steps in the search of anomalies of the flux quantization (e.g., half-integer fluxoid states [53]). Fingerprints of $\vec{d}$ texture may be also observed as a reduction in the intensity of the electron spin resonance at a characteristic frequency related to the RSOC coupling [54]. Since the $\vec{d}$ texture encodes the information of the spin of Cooper pairs, a signature of its spatial profile may manifest in the spectrum of the spin waves which couple to an applied field and it can be detected through NMR experiments [55,56]. Finally, it is well established that the generation and manipulation of quasi-1D SC topological phases require breaking of time-reversal symmetry (e.g., via magnetic fields or by proximity to ferromagnets) in order to get an effective p-wave superconductivity. In this context, although our study refers to time-reversal invariant states, the obtained results may provide interesting perspectives. On one hand, they can stimulate the search for geometric manipulation of topological states in heterostructures based on elliptically or asymmetric shaped semiconducting rings [57–62] as well as by employing suitably shaped topological insulators [63] interfaced with s-wave superconductors. On the other hand, they can lead to further investigation of topological phases with broken time-reversal symmetry and nontrivial geometry.

Acknowledgments. We acknowledge the financial support of the Future and Emerging Technologies (FET) program under FET-Open Grant No. 618083 (CNTQC). C.O. acknowledges support from the Deutsche Forschungsgemeinschaft (Grant No. OR 404/1-1) and from a VIDI grant (Project No. 680-47-543) financed by the Netherlands Organization for Scientific Research (NWO).

[1] G. Dresselhaus, Phys. Rev. **100**, 580 (1955).

[2] E. I. Rashba, Sov. Phys. Solid State **2**, 1109 (1960).

[3] Y. A. Bychkov and E. I. Rasbha, Pis'ma Zh. Eksp. Teor. Fiz. **39**, 66 (1984).

[4] L. P. Gor'kov and E. I. Rashba, Phys. Rev. Lett. **87**, 037004 (2001).
[5] P. A. Frigeri, D. F. Agterberg, A. Koga, and M. Sigrist, Phys. Rev. Lett. **92**, 097001 (2004).
[6] C.-K. Lu and S. Yip, Phys. Rev. B **78**, 132502 (2008).
[7] A. B. Vorontsov, I. Vekhter, and M. Eschrig, Phys. Rev. Lett. **101**, 127003 (2008).
[8] Y. Tanaka, T. Yokoyama, A. V. Balatsky, and N. Nagaosa, Phys. Rev. B **79**, 060505(R) (2009).
[9] M. Sato and S. Fujimoto, Phys. Rev. B **79**, 094504 (2009).
[10] R. M. Lutchyn, J. D. Sau, and S. Das Sarma, Phys. Rev. Lett. **105**, 077001 (2010).
[11] Y. Oreg, G. Refael, and F. von Oppen, Phys. Rev. Lett. **105**, 177002 (2010).
[12] V. Mourik, K. Zuo, S. M. Frolov, S. R. Plissard, E. P. A. M. Bakkers, and L. P. Kouwenhoven, Science **336**, 1003 (2012).
[13] M. T. Deng, C. L. Yu, G. Y. Huang, M. Larsson, P. Caroff, and H. Q. Xu, Nano Lett. **12**, 6414 (2012).
[14] A. Das, Y. Ronen, Y. Most, Y. Oreg, M. Heiblum, and H. Shtrikman, Nat. Phys. **8**, 887 (2012).
[15] H. O. H. Churchill, V. Fatemi, K. Grove-Rasmussen, M. T. Deng, P. Caroff, H. Q. Xu, and C. M. Marcus, Phys. Rev. B **87**, 241401(R) (2013).
[16] J. Alicea, Y. Oreg, G. Refael, F. von Oppen, and M. P. A. Fisher, Nat. Phys. **7**, 412 (2011).
[17] B. I. Halperin, Y. Oreg, A. Stern, G. Refael, J. Alicea, and F. von Oppen, Phys. Rev. B **85**, 144501 (2012).
[18] D. J. Clarke, J. D. Sau, and S. Tewari, Phys. Rev. B **84**, 035120 (2011).
[19] F. Pientka, A. Romito, M. Duckheim, Y. Oreg, and F. von Oppen, New J. Phys. **15**, 025001 (2013).
[20] B. Scharf and I. Žutíc, Phys. Rev. B **91**, 144505 (2015).
[21] B. Rosenstein, I. Shapiro, and B. Ya. Shapiro, Europhys. Lett. **102**, 57002 (2013).
[22] M. Lee, H. Khim, and M.-S. Choi, Phys. Rev. B **89**, 035309 (2014).
[23] A. Ghazaryan, A. Manaselyan, and T. Chakraborty, Phys. Rev. B **93**, 245108 (2016).
[24] D. Frustaglia and K. Richter, Phys. Rev. B **69**, 235310 (2004).
[25] H. Saarikoski, J. E. Vázquez-Lozano, J. P. Baltanás, F. Nagasawa, J. Nitta, and D. Frustaglia, Phys. Rev. B **91**, 241406(R) (2015).
[26] F. Nagasawa, D. Frustaglia, H. Saarikoski, K. Richter, and J. Nitta, Nat. Commun. **4**, 2526 (2013).
[27] Z.-J. Ying, P. Gentile, C. Ortix, and M. Cuoco, Phys. Rev. B **94**, 081406(R) (2016).
[28] P. Gentile, M. Cuoco, and C. Ortix, Phys. Rev. Lett. **115**, 256801 (2015).
[29] A. M. Turner, V. Vitelli, and D. R. Nelson, Rev. Mod. Phys. **82**, 1301 (2010).
[30] A. I. Larkin and Y. N. Ovchinnikov, J. Low Temp. Phys. **34**, 409 (1979).
[31] M. Li, Q. Song, T.-H. Liu, L. Meroueh, G. D. Mahan, M. S. Dresselhaus, and G. Chen, Nano Lett. **17**, 4604 (2017).
[32] Y. A. Ying, N. E. Staley, Y. Xin, K. Sun, X. Cai, D. Fobes, T. J. Liu, Z. Q. Mao, and Y. Liu, Nat. Commun. **4**, 2596 (2013).
[33] L. F. Chibotaru, A. Ceulemans, V. Bruyndoncx, and V. V. Moshchalkov, Nature (London) **408**, 833 (2000).
[34] J. Kim, V. Chua, G. A. Fiete, H. Nam, A. H. MacDonald, and C.-K. Shih, Nat. Phys. **8**, 464 (2012).
[35] M. J. Bowick, D. R. Nelson, and A. Travesset, Phys. Rev. B **62**, 8738 (2000).
[36] P. Gentile, M. Cuoco, and C. Ortix, SPIN **03**, 1340002 (2013).
[37] See Supplemental Material at http://link.aps.org/supplemental/10.1103/PhysRevB.96.100506 where we provide more details about the model Hamiltonian, present the phase diagram for a ring with length $L = 400a_0$ (a_0 being the lattice spacing), and the evolution of the spin-singlet order parameter for a representative case of pairing coupling for which the superconducting coherence length is comparable with the system size. We report the behavior of the coherence length as a function of the pairing coupling, the RSOC, and the chemical potential. Furthermore, the case of nanowire with sinusoidal shape is also analyzed to address the issue of having a geometrical configuration with positive and negative curvature.
[38] C. Ortix, Phys. Rev. B **91**, 245412 (2015).
[39] E. Zhang, S. Zhang, and Q. Wang, Phys. Rev. B **75**, 085308 (2007).
[40] F. E. Meijer, A. F. Morpurgo, and T. M. Klapwijk, Phys. Rev. B **66**, 033107 (2002).
[41] M. Cuoco, A. Romano, C. Noce, and P. Gentile, Phys. Rev. B **78**, 054503 (2008).
[42] We notice that, as extensively reported in Ref. [27], the geometric curvature acts as an effective spin torque and can drive topological changes for the spin texture with spatial variation of the electron spin winding. These topological transitions in the spin textures are dynamically driven by the geometric torque due to the spatial dependent curvature. The variation of the spin texture strongly influences the electrical conductance when attaching the leads to the nanoring. This is due to the effects of the spin texture on the total phase acquired by an electron when encircling the quantum loop [27].
[43] Y. Asano, Phys. Rev. B **72**, 092508 (2005).
[44] N. Read and D. Green, Phys. Rev. B **61**, 10267 (2000).
[45] G. E. Volovik, JETP Lett. **70**, 609 (1999).
[46] D. A. Ivanov, Phys. Rev. Lett. **86**, 268 (2001).
[47] S. LaShell, B. A. McDougall, and E. Jensen, Phys. Rev. Lett. **77**, 3419 (1996).
[48] Y. M. Koroteev, G. Bihlmayer, J. E. Gayone, E. V. Chulkov, S. Blügel, Ph. M. Echenique, and P. Hofmann, Phys. Rev. Lett. **93**, 046403 (2004).
[49] B. Slomski, G. Landolt, F. Meier, L. Patthey, G. Bihlmayer, J. Osterwalder, and J. H. Dil, Phys. Rev. B **84**, 193406 (2011).
[50] A. Ron and Y. Dagan, Phys. Rev. Lett. **112**, 136801 (2014).
[51] D. F. Bogorin, C.-W. Bark, H.-W. Jang, C. Cen, C. M. Folkman, C.-B. Eom, and J. Levy, Appl. Phys. Lett. **97**, 013102 (2010).
[52] C. Stephanos, M. Breitschaft, R. Jany, B. Kiessig, S. Paetel, C. Richter, and J. Mannhart, J. Phys. Soc. Jpn. **81**, 064703 (2012).
[53] J. Jang, D. G. Ferguson, V. Vakaryuk, R. Budakian, S. B. Chung, P. M. Goldbart, and Y. Maeno, Science **331**, 186 (2011).
[54] K. Maki, in *Solitons*, edited by S. E. Trullinger, V. E. Zakharov, and V. L. Pokrovkii (North-Holland, Amsterdam, 1986).
[55] M. M. Salomaa and G. E. Volovik, Phys. Rev. Lett. **55**, 1184 (1985).
[56] K. Maki, Phys. Rev. Lett. **56**, 1312 (1986).
[57] *Physics of Quantum Rings*, edited by V. M. Fomin (Springer-Verlag, Berlin/Heidelberg, 2014).

[58] R. Blossey and A. Lorke, Phys. Rev. E **65**, 021603 (2002).

[59] P. Offermans, P. M. Koenraad, J. H. Wolter, D. Granados, J. M. Garcia, V. M. Fomin, V. N. Gladilin, and J. T. Devreese, Appl. Phys. Lett. **87**, 131902 (2005).

[60] J. Wu, Z. M. Wang, K. Holmes, E. Marega, Jr., Z. Zhou, H. Li, Y. I. Mazur, and G. J. Salamo, Appl. Phys. Lett. **100**, 203117 (2012).

[61] T. Raz, D. Ritter, and G. Bahir, Appl. Phys. Lett. **82**, 1706 (2003).

[62] J. Sormunen, J. Riikonen, M. Mattila, J. Tiilikainen, M. Sopanen, and H. Lipsanen, Nano. Lett. **5**, 1541 (2005).

[63] M. König, A. Tschetschetkin, E. M. Hankiewicz, J. Sinova, V. Hock, V. Daumer, M. Schafer, C. R. Becker, H. Buhmann, and L. W. Molenkamp, Phys. Rev. Lett. **96**, 076804 (2006).